BMC Musculoskeletal Disorders

RESEARCH

Open Access

Biomechanical properties of a suture anchor system from human allogenic mineralized cortical bone matrix for rotator cuff repair

Jakob E. Schanda[1,2,3,4*], Barbara Obermayer-Pietsch[5], Gerhard Sommer[6], Philipp R. Heuberer[7,8], Brenda Laky[8], Christian Muschitz[9], Klaus Pastl[10], Eva Pastl[10], Christian Fialka[1,11], Rainer Mittermayr[1,2,3], Johannes Grillari[2,3,12] and Ines Foessl[4]

Abstract

Background: Suture anchors (SAs) made of human allogenic mineralized cortical bone matrix are among the newest developments in orthopaedic and trauma surgery. Biomechanical properties of an allogenic mineralized suture anchor (AMSA) are not investigated until now. The primary objective was the biomechanical investigation of AMSA and comparing it to a metallic suture anchor (MSA) and a bioabsorbable suture anchor (BSA) placed at the greater tuberosity of the humeral head of cadaver humeri. Additionally, we assessed the biomechanical properties of the SAs with bone microarchitecture parameters.

Methods: First, bone microarchitecture of 12 fresh frozen human cadaver humeri from six donors was analyzed by high-resolution peripheral quantitative computed tomography. In total, 18 AMSAs, 9 MSAs, and 9 BSAs were implanted at a 60° angle. All three SA systems were systematically implanted alternating in three positions within the greater tuberosity (position 1: anterior, position 2: central, position 3: posterior) with a distance of 15 mm to each other. Biomechanical load to failure was measured in a uniaxial direction at 135°.

Results: Mean age of all specimens was 53.6 ± 9.1 years. For all bone microarchitecture measurements, linear regression slope estimates were negative which implies decreasing values with increasing age of specimens. Positioning of all three SA systems at the greater tuberosity was equally distributed ($p = 0.827$). Mean load to failure rates were higher for AMSA compared to MSA and BSA without reaching statistical significance between the groups ($p = 0.427$). Anchor displacement was comparable for all three SA systems, while there were significant differences regarding failure mode between all three SA systems ($p < 0.001$). Maximum load to failure was reached in all cases for AMSA, in 44.4% for MSA, and in 55.6% for BSA. Suture tear was observed in 55.6% for MSA and in 22.2% for BSA. Anchor breakage was solely seen for BSA (22.2%). No correlations were observed between bone microarchitecture parameters and load to failure rates of all three suture anchor systems.

Conclusions: The AMSA showed promising biomechanical properties for initial fixation strength for RCR. Since reduced BMD is an important issue for patients with chronic rotator cuff lesions, the AMSA is an interesting alternative to MSA and BSA. Also, the AMSA could improve healing of the enthesis.

Keywords: Shoulder, Shoulder surgery, Rotator cuff reconstruction, Suture anchor, Allogenic mineralized suture anchor, Biomechanical analysis, High-resolution peripheral quantitative computed tomography

*Correspondence: jakob.schanda@gmail.com

[1] Department for Trauma Surgery, AUVA Trauma Center Vienna-Meidling, Vienna, Austria
Full list of author information is available at the end of the article

Background

Full-thickness rotator cuff (RC) tears are common in the general working population [1] with an increasing incidence in age [2]. Surgical RC repair (RCR) showed superior clinical outcomes compared to conservative treatment after a minimum follow-up of ten years [3]. Arthroscopic RCR using suture anchors (SAs) showed promising long-term results [4, 5]. Since bone mineral density (BMD) of the humeral head is a crucial factor for fixation strength [6–9], reduced BMD impairs bone ingrowth of SAs leading to loosening, pullout, or eventually failure of RCR [9–11]. Biomechanical properties, especially in osteoporotic bone are varying drastically according to different SA designs and materials [9, 11–14].

Despite satisfying outcomes of different SA systems, several complications are reported [15]. In case of metallic SAs, loosening [16, 17], migration within the joint [17], chondral damage [17], or resulting metallic artifacts in magnetic resonance imaging [18] are published. To overcome these complications, bioabsorbable SA systems were alternatively developed [19]. However, these novel SAs faced further complications such as synovitis due to the local resorption process [17, 20, 21], bone cyst formation [17, 21–24], or osteolysis [22, 23, 25] as well as anchor migration with concomitant chondral lesions [20, 22]. All-suture anchors promised to reduce the invasiveness and complications related to rigid SAs [26]. However, all-suture anchors are controversially discussed because of reduced biomechanical properties [27]. Since biology plays a crucial role for healing rates after RCR [28–30], an allogenic mineralized suture anchor (AMSA) may improve bone ingrowth and regeneration of the enthesis by endochondral ossification leading to higher stability after RCR [31–33].

We hypothesized that the AMSA has at least comparable biomechanical properties to a metallic SA (MSA) and a bioabsorbable SA (BSA). The primary objective was the biomechanical investigation of AMSA and comparing it to MSA and BSA placed at the greater tuberosity of the humeral head of cadaver humeri. Additionally, we assessed the biomechanical properties of the SAs with bone microarchitecture parameters.

Methods

Preparation of specimens

Six pairs of fresh frozen human cadaver humeri ($n = 12$) were donated from the tissue bank of the German Institute for Cell- and Tissue-Replacement (Deutsches Institut für Zell- und Gewebeersatz – DIZG, Berlin, Germany). Specimens were excluded if macroscopic signs of degeneration, traumatic lesions, osteoarthritis, or previous surgical interventions were present. All specimens were thawed at room temperature 24 hours before testing. In a pilot study, a total of nine AMSAs (SharkScrew® suture, surgebright, Lichtenberg, Austria) were implanted at three positions within the greater tuberosity (position 1: anterior, position 2: central, position 3: posterior) in three human cadaver humeri. In a follow-up study, a total of nine AMSAs were further compared to nine MSA (5.5 mm HEALIX TI™, DePuy Synthes, Raynham, MA, USA) and nine BSA (vented 5.5 mm BioComposite SwiveLock® Arthrex, Naples, FL, USA). All SA systems were implanted according to the manufacturer's instructions at a 60° angle as previously published [34]. For biomechanical testing, all SAs were loaded with two FiberWire® #2 sutures (Arthrex, Naples, FL, USA) [35]. All three SA systems were systematically implanted alternating in three positions within the greater tuberosity starting 10 mm posterior of the bicipital groove (position 1: anterior, position 2: central, position 3: posterior) with a distance of 15 mm to each other (Fig. 1A). Data from the pilot study and the follow-up study were merged to increase the total sample size.

Bone microarchitecture analysis

Before SA implantation, bone microarchitecture analysis of all specimens was performed by high-resolution peripheral quantitative computed tomography (HR-pQCT). Samples were placed with the greater tuberosity facing upwards within the specimen desk. All scans were performed with a Scanco Xtreme computed tomography II scanner (Scanco, Brütisellen, Switzerland). The scanner was equipped with a 60 µm spot size X-ray tube operated at 68 kVp and 100 W cone beam. The scanner was calibrated daily using a Scanco calibration phantom (Scanco, Brütisellen, Switzerland). Scans were performed with 68 kVp and 1470 µA with 900 projections of 100 ms at a voxel size and slice increment of 60.7 µm. For every specimen, a total of 638–838 slices were scanned. Segmentation settings were chosen with a Gauss-sigma of 0.8, a Gauss-support of 1, a lower threshold of 107, and an upper threshold of 1000. Cortical bone microstructure was defined by cortical thickness (Ct.Th, µm). Trabecular bone microstructure parameters included bone volume fraction (bone volume/total volume [BV/TV], %), trabecular number (Tb.N, mm^{-1}), trabecular thickness (Tb.Th, mm), BMD of bone volume (BV) (hydroxyapatite [HA]/cm^3), and BMD of total volume (TV) (HA/cm^3).

Biomechanical analysis

All specimens were fixed to a uniaxial spindle-operated testing machine (Messphysik Materials Testing, Fürstenfeld, Austria) with an adjustable fixation device. The sutures of the SAs were fixed using the Tennessee slider knot [35] and the loop of the sutures was attached to a

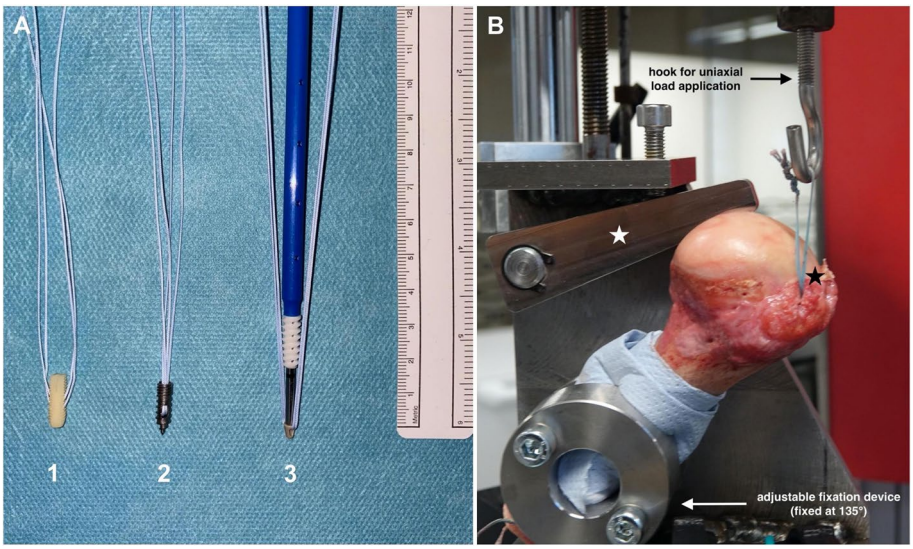

Fig. 1 Suture anchors and biomechanical setup. **A** Suture anchors tested in the study. 1: allogenic mineralized suture anchor (SharkScrew® suture), 2: metallic suture anchor (HEALIX TI™), 3: bioabsorbable suture anchor (BioComposite SwiveLock®). **B** The humerus is fixed in the uniaxial spindle-operated testing machine. The adjustable fixation device and the transversal bar (white star) prevent slipping and sliding of the specimen during biomechanical testing. The suture anchor is fixed at the greater tuberosity of the humeral head (black star) and the sutures of the anchor are knotted together and fixed on a hook for uniaxial testing at 135°

hook of the testing machine with a gauge of 30 mm to the anchor. To prevent slipping or sliding of the humeral shaft from the adjustable fixation device, the humeral head was additionally fixed with a transversal bar (Fig. 1B). The operating protocol for biomechanical testing was performed as previously reported [36] at a pulling direction of 135° [9, 36]: Initially, 50 cycles with tensile loads of 75 N were applied with a crosshead extension rate of 20 mm per minute. For the next 50 cycles, the tensile load was increased by 25 N until reaching 100 N. Then, additional increase of the tensile loads by 25 N was applied until failure of the SA system [36]. During biomechanical testing, load and displacement were permanently controlled and measured using the software "Kunststoffzugversuch" version 2.10.01 (Messphysik Materials Testing, Fürstenfeld, Austria). To ensure an accurate documentation of failure mode, video analysis was performed throughout biomechanical testing using a Sony DSC-RX10 M3 camera (Sony, Tokio, Japan). Anchor displacement (mm), anchor breakage, and suture tear were documented.

SharkScrew® suture – human allogenic mineralized cortical bone matrix

The AMSAs are manufactured in cooperation with the German Institute for Cell- and Tissue-Replacement (Deutsches Institut für Zell- und Gewebeersatz – DIZG, Berlin, Germany) according to the German Tissue Law (GewebeG, as by 2021). The AMSA is carved and the thread is reamed out of a cortical bone block harvested from the femur of tissue-donors. The SA has a length of 15 mm with a diameter of 5 mm. The AMSA is decellularized and sterilized using a peracetic acid-methanol mixture, to ensure a reduction of bacteria and viruses below the detection levels [37, 38]. Microscopically, the AMSA consists of mineralized osteons with surrounding lamellae and central Haversian canals (Fig. 2).

Statistical analysis

Descriptive statistics was used to present the specimens' characteristics. Distribution of the data was assessed by a visual inspection of histograms and the Kolmogorov-Smirnov-test. Normally distributed continuous data are presented as mean with standard deviation, otherwise as median and range. Categorical variables are described as proportions and frequency counts. Scatterplots including linear regression lines were used to visualize bone microarchitecture parameters with age. Categorial data were assessed using Fisher's exact test. Kruskal-Wallis tests were used for comparison between the three SA systems. Spearman's correlation coefficients (rho) were used to explore correlations between continuous parameters.

All tests were two-sided and p-values less than 0.05 were considered as statistically significant. All statistical analyses were performed with the statistical software SPSS (IMP Statistics Version 25; SPSS Inc., Chicago, IL).

An a-priori Power Analysis was performed using G*Power software version 3.1.9.2 (Heinrich Heine University, Düsseldorf, Germany). According to a previous

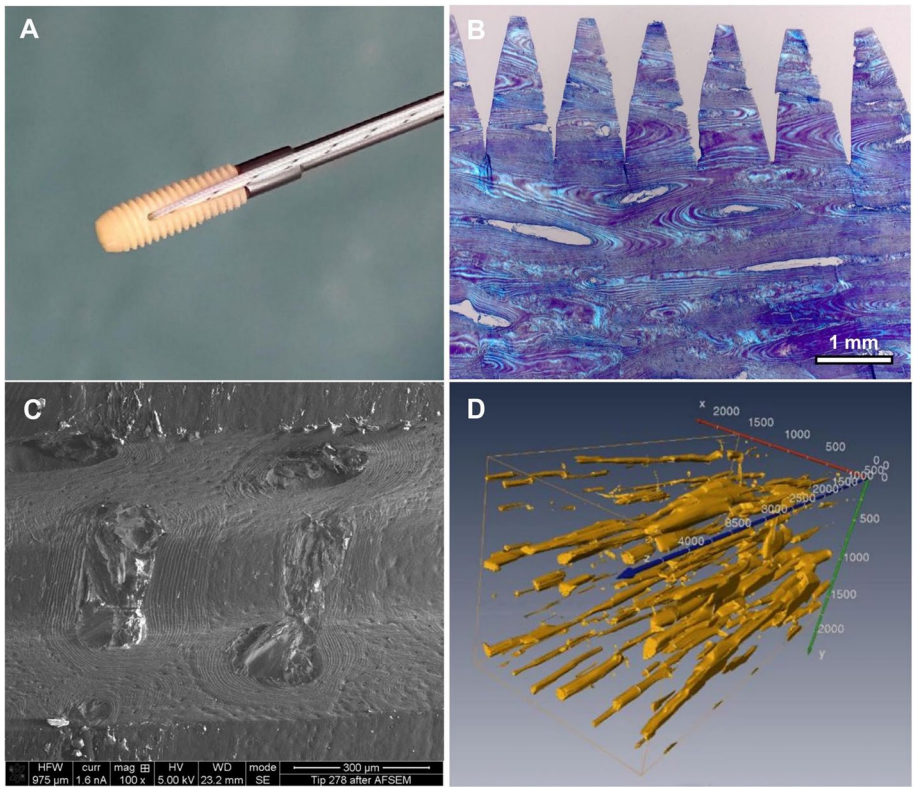

Fig. 2 Structure of the SharkScrew® suture, an allogenic mineralized suture anchor (AMSA). **A** The AMSA is armed with two FiberWire® #2 sutures and fixed on the implantation screwdriver. **B** Histological section of a sterile AMSA (toluidine blue staining) under fluorescent light. Decellularized and mineralized osteons with the surrounding lamellae and central Harversian canals are visible. **C** Electron microscopic image of the AMSA. Decellularized Harversian canals with surrounding bone lamellae are visible. **D** Animation of the AMSA after subtraction of bone tissue. The Harversian canal system is visible all along the suture anchor

biomechanical study investigating maximum load to failure rates of SAs in human cadaver humeri [26], a sample size of nine would achieve a significance level (α) of 0.05 and a power of 80%.

Results

Mean age of all specimens was 53.6 ± 9.1 years. For all bone microarchitecture measurements, linear regression slope estimates are negative which implies decreasing values with increasing age of specimens. None of the slope estimates showed statistical significance (Fig. 3).

Positioning of all three SA systems at the greater tuberosity was equally distributed ($p = 0.827$). Mean load to failure rates were higher for AMSA compared to MSA, and BSA without reaching statistical significance between the groups ($p = 0.427$). Anchor displacement was comparable for all three SA systems, while there were significant differences regarding failure mode between all three SA systems ($p < 0.001$). Maximum load to failure was reached in all cases for AMSA, in 44.4% for MSA, and in 55.6% for BSA. Suture tear was observed in 55.6% for MSA and in 22.2% for BSA. Anchor breakage was solely seen for BSA (22.2%) (Table 1). Comparable load to failure and anchor displacement were observed between SA systems for every implantation position (Fig. 4, Table 2). No correlations were observed between bone microarchitecture parameters and load to failure rates of all three SA systems (Table 3).

Discussion

This study is the first to present a novel SA system consisting of human allogenic mineralized cortical bone matrix. The AMSA provides comparable load to failure rates to a MSA or a BSA. Failure mode showed significant differences between all three SA systems. Maximum load to failure was detected in all cases with AMSA. Suture tear was recorded in five cases with MSA and in two cases with BSA. Anchor breakage was solely observed with BSA in two cases. The novel AMSA is a safe implant for RCR, even in case of osteoporotic changes on the humeral head which are commonly observed in case of chronic RC lesions.

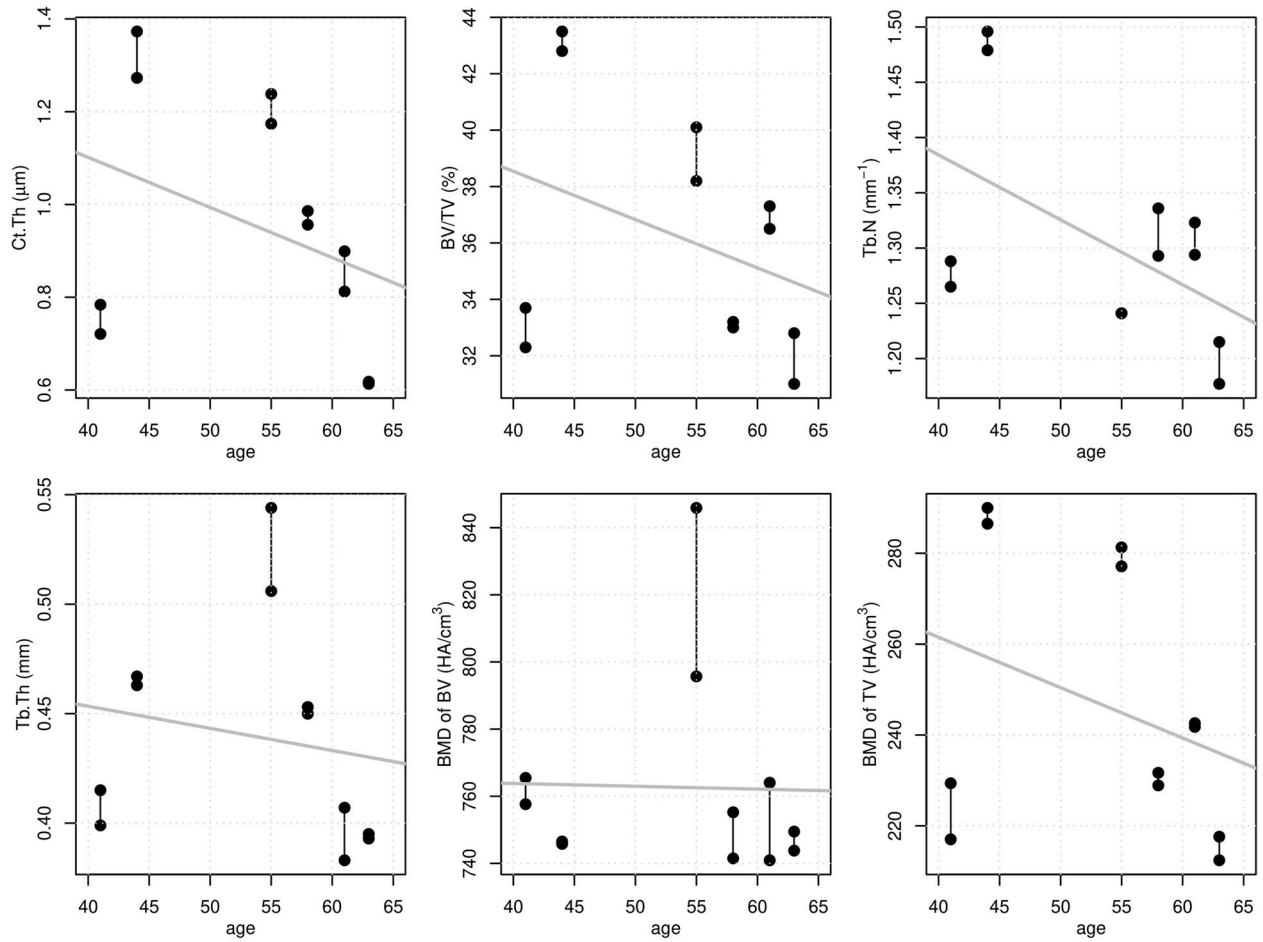

Fig. 3 Relationships between bone microarchitecture measurements and age. Pairs of measurements of humeri from identical specimen (black dots) are connected by vertical black lines. Gray lines indicated linear regressions. Slope estimates are non-significant for all measurements

Table 1 Biomechanical analysis of the allogenic mineralized suture anchor (AMSA), the metallic suture anchor (MSA), and the bioabsorbable suture anchor (BSA) at the greater tuberosity of the humeral head

	AMSA (*n* = 18)	**MSA (*n* = 9)**	**BSA (*n* = 9)**	***p*-value**
Median load to failure (N)	248 (109–467)	204 (174–371)	197 (98–330)	0.427[a]
Median anchor displacement (mm)	1.5 (1–7)	2 (1–4)	1 (0–3)	0.193[b]
Failure mode (n)				
• Anchor breakage	0 (0%)	0 (0%)	2 (22.2%)	
• Suture tear	0 (0%)	5 (55.6%)	2 (22.2%)	< 0.001[b]
• Maximum load to failure	18 (100%)	4 (44.4%)	5 (55.6%)	

[a] Kruskal-Wallis test

[b] Fisher's exact test

Since incidences of RC lesions [1, 2] as well as osteoporosis [39] are increasing with age, RCR faces a challenging problem regarding bone ingrowth of SAs and healing of the enthesis [6, 8, 11, 14]. Impaired ingrowth of SAs or healing of the enthesis consequently lead to loosening, pullout, or failure of RCR [9–11]. To improve biomechanical properties of the initial SA fixation, local SA augmentation techniques using polymethylmethacrylate [40–42], bone cement [42, 43], or calcium phosphate [42, 44, 45] are published. However, such augmentation techniques

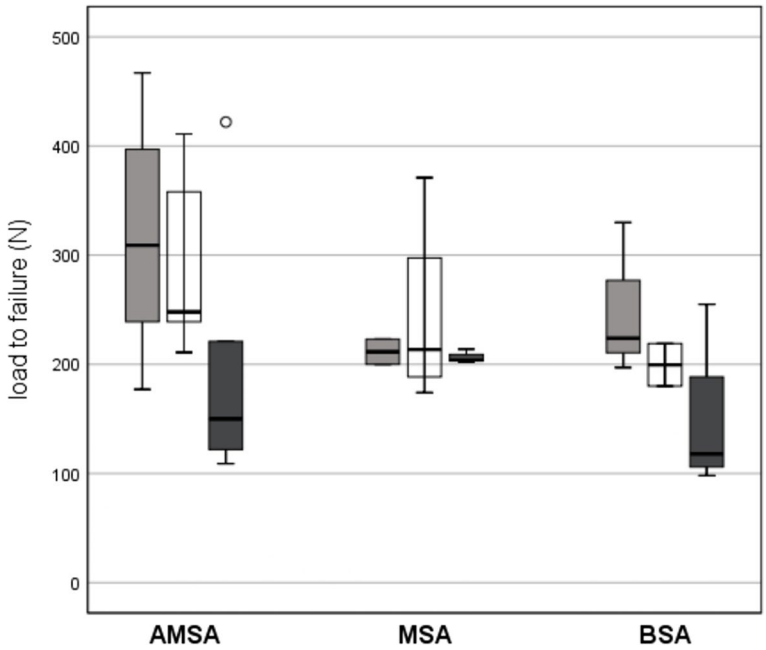

Fig. 4 Box plot diagram of load to failure. Load to failure rates are given according to the implanting position at the greater tuberosity of the humeral head (light grey: position 1 anterior; white: position 2 central; dark grey: position 3 posterior) of the allogenic mineralized suture anchor (AMSA), the metallic suture anchor (MSA), and the bioabsorbable suture anchor (BSA)

Table 2 Biomechanical analysis of the allogenic mineralized suture anchor (AMSA), the metallic suture anchor (MSA), and the bioabsorbable suture anchor (BSA) at all three implantation positions of the humeral head

	AMSA (*n* = 18)	**MSA (*n* = 9)**	**BSA (*n* = 9)**	***p*-value (between suture anchor systems)[a]**
Position 1 (anterior)				
Number of implantations	7	2	3	
Median load to failure (N)	309 (177–467)	212 (200–223)	224 (197–330)	0.419
Median anchor displacement (mm)	1 (1–2)	3 (2–4)	2 (1–2)	0.104
Position 2 (central)				
Number of implantations	6	4	2	
Median load to failure (N)	248 (211–411)	214 (174–371)	200 (180–219)	0.180
Median anchor displacement (mm)	1 (1–3)	2 (1–3)	1 (1–1)	0.347
Position 3 (posterior)				
Number of implantations	5	3	4	
Median load to failure (N)	150 (109–422)	204 (174–371)	118 (98–255)	0.497
Median anchor displacement (mm)	2 (2–7)	1 (1–3)	2 (0–3)	0.409
***p*-value (between positions regarding)[a]**				
· Load to failure	0.214	0.885	0.247	
· Anchor displacement	0.058	0.417	0.606	

[a] Kruskal-Wallis test

are not commonly performed in clinical practice [46]. An interesting and promising approach to address bone cyst formation in case of chronic degenerative RC lesions is additional autologous or allogenic bone grafting during RCR to improve the fixation strength and ingrowth of SAs. Even if satisfying results are reported throughout the literature, only a few cases of concomitant bone grafting and RCR are published [47–50].

Table 3 Spearman correlation coefficients for load to failure (N) with bone microarchitecture parameters from high-resolution peripheral quantitative computed tomography including allogenic mineralized suture anchor (AMSA), metallic suture anchor (MSA), and bioabsorbable suture anchor (BSA)

	AMSA		MSA		BSA	
	rho	p-value	rho	p-value	rho	p-value
Ct.Th (mm)	−0.072	0.777	0.500	0.170	−0.600	0.088
BV/TV (%)	−0.033	0.896	0.467	0.205	−0.333	0.381
Tb.N (mm^{-1})	−0.065	0.796	0.460	0.213	−0.100	0.797
Tb.Th (mm)	−0.104	0.682	0.367	0.332	−0.533	0.139
BMD of TV (HA/cm^3)	0.012	0.961	0.450	0.224	−0.417	0.265
BMD of BV (HA/cm^3)	0.025	0.922	0.400	0.286	−0.333	0.381

BV bone volume, *BV/TV* bone volume fraction (bone volume/total volume), *BMD* bone mineral density, *Ct. Th* cortical thickness, *HA* hydroxyapatite, *Tb. N* trabecular number, *Tb. Th* trabecular thickness, *TV* total volume

To enhance healing and regeneration of the enthesis, several authors focused on systemic antiresorptive therapies following RCR using bisphosphonates [51], recombinant human parathyroid hormone [52–54], or a sclerostin antibody [55]. However, such adjuvant systemic therapies need optimal timing for initiation and duration of these medications prior to RC surgery. To improve tendon-bone healing after RCR, augmentation techniques using demineralized bone matrix (DBM) showed promising results [56]. DBM is an osteoinductive agent consisting of a collagen scaffold and several growth factors, most importantly bone morphogenetic proteins [57]. The positive effects of allogenic, mineralized, cortical bone screws were recently confirmed in first clinical studies on hand and foot surgery [31–33]. In all cases, the authors reported of bony consolidation with remodeling of the implant and a concomitant high satisfaction rate at one year follow-up [33]. No adverse events as non-union or infection were observed [32, 33]. Histological analysis revealed vascularization of the graft with newly formed compact lamellar bone exactly fitting to the implant, plump osteoblasts with osteoid production, and osteocytes within the lacunae of the graft [31]. The novel AMSA therefore presents a biological alternative to MSAs or BSAs with an additional osteoconductive and osteoinductive potential.

So far, metallic voluminous screw-type anchors without sharp edges seem to have the highest maximum load to failure [8, 36]. However, this study showed comparable load to failure of AMSA to MSA. Even after exclusion of samples where suture tear was observed, no differences in maximum load to failure rates were observed between all three SA systems. Because of the potential biologically active characteristics of the AMSA, enhanced biomechanical properties can be expected over time due to improved bone ingrowth. In case of revision after RCR using the AMSA, no removal of previously inserted SAs is necessary and can easily be overdrilled. Also, the AMSA can be seen as augmentation graft within the humeral head, an important benefit especially in patients with reduced BMD within the humeral head.

Previously to biomechanical testing, all specimens underwent bone microarchitecture analysis by means of HR-pQCT, a non-invasive visualization of bone morphology. Similar to previous research [58, 59], this study shows a decrease in bone microarchitecture with increasing age. A reduction of BV/TV was also observed at the humeral head with increased age [60]. However, this was only reported in an older cohort with osteoporotic bone [60]. This study demonstrates a decreased bone microarchitecture in a population of peri- and postmenopausal women and similarly aged men which may rather be accessible for RCR [61].

The major limitation of this study is owed to the biomechanical setting. As solely the pullout strength of SAs from bone were analyzed, the suture-tendon-interface was not addressed in this study. Also, biological properties of bone ingrowth of the used implants and healing properties of the enthesis could not be addressed. However, since allogenic bone ingrowth at the greater tuberosity is reported in patients undergoing RCR [47–50] and DBM improves healing properties of the enthesis [56], long-term stability of the AMSA can be assumed. Moreover, even if HR-pQCT measurements were carried out previously to biomechanical testing in every specimen, no specific regions of interest were set at the humeral head for better comparability.

Conclusions

In conclusion, the AMSA showed promising biomechanical properties for initial fixation strength for RCR. Since reduced BMD is an important issue for patients with chronic RC lesions, the AMSA is an interesting alternative to MSA and BSA. Also, the AMSA could improve healing of the enthesis.

Abbreviations
AMSA: Allogenic mineralized suture anchor; BMD: Bone mineral density; BSA: Bioabsorbable suture anchor; BV: Bone volume; BV/TV: Bone volume/total volume; Ct.Th: Cortical thickness; DBM: Demineralized bone matrix; HR-pQCT: High-resolution peripheral quantitative computed tomograhy; MSA: Metallic suture anchor; RC: Rotator cuff; RCR: Rotator cuff repair; SA: Suture anchor; Tb.N: Trabecular number; Tb.Th: Trabecular thickness; TV: Total volume.

Supplementary Information

The online version contains supplementary material available at https://doi.org/10.1186/s12891-022-05371-0.

Additional file 1: Supplemental Table 1. Bone microarchitecture and bone mineral density assessment and biomechanical analysis of the allogenic mineralized suture anchor (AMSA), the metallic suture anchor (MSA), and the bioabsorbable suture anchor (BSA) at the greater tuberosity of the humeral head. Fields marked in grey are the results of the pilot study, fields marked in white are the results of the follow-up study.

Acknowledgements
Not applicable.

Authors' contributions
Study design: JES, BOP, GS, PRH, KP, EP, IF. Study conduct: BOP, GS, IF; Data collection: BOP, GS; IF. Data analysis and statistical calculations: JES, PRH, BL, CM, CF, RM, JG. Data interpretation: JES, PRH, BL, CM, CF, RM, JG. Drafting manuscript: JES, PRH, BL, CM. Approving final version of manuscript: all authors. JES takes responsibility for the integrity of the data analysis.

Funding
The study was financially supported by the Austrian Funding Research Society (Österreichische Forschungsförderungsgesellschaft, FFG), the independent national funding institution for research and development (Project Number 870203). Neither the company manufacturing the SharkScrew® suture (surgebright, Lichtenberg, Austria) or both co-authors affiliated to surgebright (KP, EP) had insight in data assessment and/or interpretation. All authors approved the final manuscript.

Availability of data and materials
The datasets used and analyzed during the current study are available from the corresponding author on reasonable request.

Declarations

Ethics approval and consent to participate
Tissue grafts in Germany are regulated as medicinal products under the German Medicinal Products Act (Arzneimittelgesetz, AMG). All tissues are acquired from non-profit tissue donation organizations after informed consent and according to the AMG and to the Transplantation Act (Transplantationsgesetz, TPG) regulations. All specimens used in this study were provided by the tissue bank of the German Institute for Cell- and Tissue-Replacement (Deutsches Institut für Zell- und Gewebeersatz – DIZG, Berlin, Germany).

Consent for publication
Not applicable.

Competing interests
KP is Chief Executive Officer and Medical Director of surgebright. EP is Vice Medical Director of surgebright. JES, BOP, GS, PRH, BL, CM, CF, RM, JG, IF certify that he or she have no commercial associations (e.g., consultancies, stock ownership, equity interest, patent/licensing arrangements, etc.) that might pose a conflict of interest in connection with the submitted article.

Author details
[1]Department for Trauma Surgery, AUVA Trauma Center Vienna-Meidling, Vienna, Austria. [2]Ludwig Boltzmann Institute for Traumatology, The Research Center in Cooperation with AUVA, Vienna, Austria. [3]Austrian Cluster for Tissue Regeneration, Vienna, Austria. [4]Michael Ogon Laboratory for Orthopaedic Research, Vienna, Austria. [5]Department of Internal Medicine, Division of Endocrinology and Diabetology, Medical University of Graz, Graz, Austria. [6] Institute of Biomechanics, Graz University of Technology, Graz, Austria. [7]healthPi Medical Center, Vienna, Austria. [8]Austrian Research Group for Regenerative and Orthopedic Medicine (AURROM), Vienna, Austria. [9]II Medical Department, Vinforce, St. Vincent Hospital Vienna, Vienna, Austria. [10]surgebright GmbH, Lichtenberg, Austria. [11] Department of Traumatology, Sigmund Freud Medical University Vienna, Vienna, Austria. [12]Institute of Molecular Biotechnology, Department of Biotechnology, University of Natural Resources and Life Science (BOKU), Vienna, Austria.

Received: 12 September 2021 Accepted: 25 April 2022
Published online: 05 May 2022

References

1. Minagawa H, Yamamoto N, Abe H, Fukuda M, Seki N, Kikuchi K, et al. Prevalence of symptomatic and asymptomatic rotator cuff tears in the general population: from mass-screening in one village. J Orthop. 2013;10:8–12.
2. Teunis T, Lubberts B, Reilly BT, Ring D. A systematic review and pooled analysis of the prevalence of rotator cuff disease with increasing age. J Shoulder Elb Surg. 2014;23:1913–21.
3. Moosmayer S, Lund G, Seljom US, Haldorsen B, Svege IC, Hennig T, et al. At a 10-year follow-up, tendon repair is superior to physiotherapy in the treatment of small and medium-sized rotator cuff tears. J Bone Joint Surg Am. 2019;101-A:1050–60.
4. Collin P, Colmar M, Thomazeau H, Mansat P, Boileau P, Valenti P, et al. Clinical and MRI outcomes 10 years after repair of massive Posterosuperior rotator cuff tears. J Bone Joint Surg Am. 2018;100-A:1854–63.
5. Heuberer PR, Smolen D, Pauzenberger L, Plachel F, Salem S, Laky B, et al. Longitudinal long-term magnetic resonance imaging and clinical follow-up after single-row arthroscopic rotator cuff repair clinical superiority of structural tendon integrity. Am J Sports Med. 2017;45:1283–8.
6. Barber FA, Feder SM, Burkhart SS, Ahrens J. The relationship of suture anchor failure and bone density to proximal Humerus location: a cadaveric study. Arthroscopy. 1997;13:340–5.
7. Meyer DC, Fucentese SF, Koller B, Gerber C. Association of osteopenia of the humeral head with full-thickness rotator cuff tears. J Shoulder Elb Surg. 2004;13:333–7.
8. Tingart MJ, Apreleva M, Lehtinen J, Zurakowski D, Warner JJP. Anchor design and bone mineral density affect the pull-out strength of suture anchors in rotator cuff repair which anchors are best to use in patients with low bone quality? Am J Sports Med. 2004;32:1466–73.
9. Tingart MJ, Apreleva M, Zurakowski D, Warner JJP. Pullout strength of suture anchors used in rotator cuff repair. J Bone Joint Surg Am. 2003;85-A:2190–8.
10. Chung SW, Oh JH, Gong HS, Kim JY, Kim SH. Factors affecting rotator cuff healing after arthroscopic repair osteoporosis as one of the independent risk factors. Am J Sports Med. 2011;39:2099–107.
11. Horoz L, Hapa O, Barber FA, Hüsemoğlu B, Özkan M, Havitçioğlu H. Suture anchor fixation in osteoporotic bone: a biomechanical study in an ovine model. Arthroscopy. 2017;33:68–74.
12. Chae S, Kang J, Lee J, Han S, Kim S. Effect of structural design on the pullout strength of suture anchors for rotator cuff repair. J Orthop Res. 2018;36:3318–27.
13. McFarland EG, Park HB, Keyurapan E, Gill HS, Selhi HS. Suture anchors and tacks for shoulder surgery, part 1. Am J Sports Med. 2005;33:1918–23.
14. Pietschmann MF, Fröhlich V, Ficklscherer A, Gülecyüz MF, Wegener B, Jansson V, et al. Suture anchor fixation strength in osteopenic versus non-osteopenic bone for rotator cuff repair. Arch Orthop Trauma Surg. 2009;129:373–9.
15. Visscher LE, Jeffery C, Gilmour T, Anderson L, Couzens G. The history of suture anchors in orthopaedic surgery. Clin Biomech. 2019;61:70–8.
16. Kaar TK, Schenck RC, Wirth MA, Rockwood CA. Complications of metallic suture anchors in shoulder surgery: a report of 8 cases. Arthroscopy. 2001;17:31–7.
17. Ma R, Chow R, Choi L, Diduch D. Arthroscopic rotator cuff repair: suture anchor properties, modes of failure and technical considerations. Expert Med Rev Devices. 2011;8:377–87.

18. Gaenslen ES, Satterlee CC, Hinson GW. Magnetic resonance imaging for evaluation of failed repairs of the rotator cuff relationship to operative findings. J Bone Joint Surg Am. 1996;78-A:1391–6.
19. Ozbaydar M, Elhassan B, Warner JJP. The use of anchors in shoulder surgery: a shift from metallic to bioabsorbable anchors. Arthroscopy. 2007;23:1124–6.
20. McCarty LPI, Buss DD, Datta MW, Freehill MQ, Giveans MR. Complications observed following labral or rotator cuff repair with use of poly-L-lactic acid implants. J Bone Joint Surg Am. 2013;95-A:507–11.
21. Nusselt T, Freche S, Klinger H-M, Baums MH. Intraosseous foreign body granuloma in rotator cuff repair with bioabsorbable suture anchor. Arch Orthop Traum Surg. 2010;130:1037–40.
22. Dhawan A, Ghodadra N, Karas V, Salata MJ, Cole BJ. Complications of bioabsorbable suture anchors in the shoulder. Am J Sports Med. 2012;40:1424–30.
23. Haneveld H, Hug K, Diederichs G, Scheibel M, Gerhardt C. Arthroscopic double-row repair of the rotator cuff: a comparison of bio-absorbable and non-resorbable anchors regarding osseous reaction. Knee Surg Sports Traumatol Arthrosc. 2013;21:1647–54.
24. Kim SH, Kim DY, Kwon JE, Park JS, Oh JH. Perianchor cyst formation around biocomposite biodegradable suture anchors after rotator cuff repair. Am J Sports Med. 2015;43:2907–12.
25. Vonhoegen J, John D, Hägermann C. Osteoconductive resorption characteristics of a novel biocomposite suture anchor material in rotator cuff repair. J Orthop Surg Res. 2019;14(1):12.
26. Oh JH, Jeong HJ, Yang SH, Rhee SM, Itami Y, McGarry MH, et al. Pullout strength of all-suture anchors: effect of the insertion and traction angle––a biomechanical study. Arthroscopy. 2018;34:2784–95.
27. Nagra NS, Zargar N, Smith RDJ, Carr AJ. Mechanical properties of all-suture anchors for rotator cuff repair. Bone Joint Res. 2017;6:82–9.
28. Dierckman BD, Ni JJ, Karzel RP, Getelman MH. Excellent healing rates and patient satisfaction after arthroscopic repair of medium to large rotator cuff tears with a single-row technique augmented with bone marrow vents. Knee Surg Sports Traumatol Arthrosc. 2018;26:136–45.
29. Lorbach O, Tompkins M. Rotator cuff: biology and current arthroscopic techniques. Knee Surg Sports Traumatol Arthrosc. 2012;20:1003–11.
30. Lorbach O, Baums MH, Kostuj T, Pauly S, Scheibel M, Carr A, et al. Advances in biology and mechanics of rotator cuff repair. Knee Surg Sports Traumatol Arthrosc. 2015;23:530–41.
31. Brcic I, Pastl K, Plank H, Igrec J, Schanda JE, Pastl E, et al. Incorporation of an allogenic cortical bone graft following arthrodesis of the first metatarsophalangeal joint in a patient with hallux Rigidus. Life. 2021;11(1):473.
32. Huber T, Hofstätter SG, Fiala R, Hartenbach F, Breuer R, Rath B. The application of an allogenic bone screw for stabilization of a modified Chevron osteotomy: a prospective analysis. J Clin Med. 2022;11(1):1384.
33. Pastl K, Schimetta W. The application of an allogeneic bone screw for osteosynthesis in hand and foot surgery: a case series. Arch Orthop Trauma Surg. 2021. https://doi.org/10.1007/s00402-021-03880-6.
34. Burkhart SS. The Deadman theory of suture anchors: observations along a South Texas fence line. Arthroscopy. 1995;11:119–23.
35. Barber FA, Herbert MA, Beavis RC. Cyclic load and failure behavior of arthroscopic knots and high strength sutures. Arthroscopy. 2009;25:192–9.
36. Schneeberger AG, von RA, Kalberer F, Jacob HAC, Gerber C. Mechanical strength of arthroscopic rotator cuff repair techniques a in vitro study. J Bone Joint Surg Am. 2002;84-A:2152–60.
37. Pruss A, Baumann B, Seibold M, Kao M, Tintelnot K, R von V, et al. Validation of the sterilization procedure of allogeneic avital bone transplants using Peracetic acid-ethanol. Biologicals. 2001;29:59–66.
38. Pruss A, Kao M, Kiesewetter H, Versen RV, Pauli G. Virus safety of avital bone tissue transplants: evaluation of sterilization steps of Spongiosa cuboids using a Peracetic acid-methanol mixture. Biologicals. 1999;27:195–201.
39. Compston JE, McClung MR, Leslie WD. Osteoporosis Lancet. 2019;393:364–76.
40. Braunstein V, Ockert B, Windolf M, Sprecher CM, Mutschler W, Imhoff A, et al. Increasing pullout strength of suture anchors in osteoporotic bone using augmentation–a cadaver study. Clin Biomech. 2015;30:243–7.
41. Giori NJ, Sohn DH, Mirza FM, Lindsey DP, Lee AT. Bone cement improves suture anchor fixation. Clin Orthop Relat Res. 2006;451:236–41.
42. Er MS, Altinel L, Eroglu M, Verim O, Demir T, Atmaca H. Suture anchor fixation strength with or without augmentation in osteopenic and severely osteoporotic bones in rotator cuff repair: a biomechanical study on polyurethane foam model. J Orthop Surg Res. 2014;9(1):48.
43. Aziz KT, Shi B, Okafor L, Smalley J, Belkoff SM, Srikumaran U. Pullout strength of standard vs. cement-augmented rotator cuff repair anchors in cadaveric bone. Clin Biomech. 2018;54:132–6.
44. Diaz MA, Branch EA, Paredes LA, Oakley E, Baker CE. Calcium phosphate bone void filler increases threaded suture anchor pullout strength: a biomechanical study. Arthroscopy. 2020;36:1000–8.
45. Oshtory R, Lindsey DP, Giori NJ, Mirza FM. Bioabsorbable Tricalcium phosphate bone cement strengthens fixation of suture anchors. Clin Orthop Relat Res. 2010;468:3406–12.
46. Truntzer JN, Giori NJ, Saleh JR. Editorial commentary: augmenting suture anchor fixation: why has it not caught on? Arthroscopy. 2020;36:1009–10.
47. Agrawal V, Stinson M. Arthroscopic grafting of greater tuberosity cyst and rotator cuff repair. Arthroscopy. 2007;23:904.e1–3.
48. Burkhart SS, Klein JR. Arthroscopic repair of rotator cuff tears associated with large bone cysts of the proximal Humerus: compaction bone grafting technique. Arthroscopy. 2005;21:1149.e1–5.
49. Kim KC, Rhee KJ, Shin HD, Kim YM. Arthroscopic footprint reconstruction of a bone cyst-associated rotator cuff tear. Knee Surg Sports Traumatol Arthrosc. 2007;15:1486–8.
50. Levy DM, Moen TC, Ahmad CS. Bone grafting of humeral head cystic defects during rotator cuff repair. Am J Orthop (Belle Mead NJ). 2012;41:92–4.
51. Schanda JE, Keibl C, Heimel P, Monforte X, Tangl S, Feichtinger X, et al. Zoledronic acid substantially improves bone microarchitecture and biomechanical properties after rotator cuff repair in a rodent chronic defect model. Am J Sports Med. 2020;48:2151–60.
52. Duchman KR, Goetz JE, Uribe BU, Amendola AM, Barber JA, Malandra AE, et al. Delayed administration of recombinant human parathyroid hormone improves early biomechanical strength in a rat rotator cuff repair model. J Shoulder Elb Surg. 2016;25:1280–7.
53. Hettrich CM, Beamer BS, Bedi A, Deland K, Deng X-H, Ying L, et al. The effect of rhPTH on the healing of tendon to bone in a rat model. J Orthop Res. 2012;30:769–74.
54. Oh JH, Kim DH, Jeong HJ, Park JH, Rhee S-M. Effect of recombinant human parathyroid hormone on rotator cuff healing after arthroscopic repair. Arthroscopy. 2019;35:1064–71.
55. Shah SA, Kormpakis I, Havlioglu N, Ominsky MS, Galatz LM, Thomopoulos S. Sclerostin antibody treatment enhances rotator cuff tendon-to-bone healing in an animal model. J Bone Joint Surg Am. 2017;99-A:855–64.
56. Hexter AT, Pendegrass C, Haddad F, Blunn G. Demineralized bone matrix to augment tendon-bone healing a systematic review. Orthop. J Sports Med. 2017;5(1):2325967117734517.
57. Urist MR. Bone: formation by autoinduction. Science. 1965;150:893–9.
58. Burt LA, Hanley DA, Boyd SK. Cross-sectional versus longitudinal change in a prospective HR-pQCT study. J Bone Miner Res. 2017;32:1505–13.
59. Samelson EJ, Broe KE, Xu H, Yang L, Boyd S, Biver E, et al. Cortical and trabecular bone microarchitecture as an independent predictor of incident fracture risk in older women and men in the bone microarchitecture international consortium (BoMIC): a prospective study. Lancet Diabetes Endocrinol. 2018;7:34–43.
60. Kirchhoff C, Braunstein V, Milz S, Sprecher CM, Fischer F, Tami A, et al. Assessment of bone quality within the Tuberosities of the osteoporotic humeral head relevance for anchor positioning in rotator cuff repair. Am J Sports Med. 2010;38:564–9.
61. Moraiti C, Valle P, Maqdes A, Boughebri O, Dib C, Giakas G, et al. Comparison of functional gains after arthroscopic rotator cuff repair in patients over 70 years of age versus patients under 50 years of age: a prospective multicenter study. Arthroscopy. 2015;31:184–90.

Publisher's Note